J Soils Sediments
DOI 10.1007/s11368-015-1185-4

Flood bench chronology and sediment source tracing in the upper Thina catchment, South Africa: the role of transformed landscape connectivity

Bennie van der Waal[1] · **Kate Rowntree**[1] · **Simon Pulley**[1]

Received: 25 March 2015 / Accepted: 15 June 2015

Abstract
Purpose Sediment pressures can be increased by transformed landscape connectivity in catchments worldwide. The upper Thina catchment, an important high rainfall water resource in the northern Eastern Cape, South Africa, is used to explore how ongoing subsistence farming on communal land (overgrazing and trampling) has initiated large erosive features and increased sediment loads.
Materials and methods The headwaters of the Thina catchment are underlain by igneous parent lithology and the lower catchment by sedimentary rock lithology, making it ideal for sediment tracing using mineral magnetic signatures. Floodplain cores were dated using ^{210}Pb and ^{137}Cs techniques, and core sediment was traced to hillslope sources using quantitative (unmixing model) and semi-qualitative approaches.
Results and discussion Sediment accumulation rates varied between 0.2 and 3.3 g cm^{-2} year^{-1} (92+years old) for the higher flood benches and 0.6 and 11 g cm^{-2} year^{-1} (46–60 years old) for the lower flood benches. It was found that a semi-qualitative approach based on low-frequency magnetic susceptibility (Xlf) could be used to effectively trace and apportion sediment in a catchment with strongly contrasting lithologies. The tracing results showed that over the past century the dominant sediment source for flood benches has been local sedimentary rock sources, with upstream igneous rock sources making a smaller contribution. It is proposed that igneous rock-dominated sediment from the upper catchment is temporarily stored until larger events transport it to the lower catchment.
Conclusions Sediment stored in flood benches was mostly from the adjacent sedimentary rock sources despite the larger area of the igneous formation in the catchment. This shows the vulnerability of the sedimentary formation to land use change and pressures.

Keywords Contrasting lithologies · Floodplain cores · Mineral magnetic fingerprinting · Radionuclide dating · Sediment tracing · Umzimvubu catchment

Responsible editor: Ian Foster

✉ Bennie van der Waal
bvdwaal@gmail.com

[1] Geography Department, Rhodes University, Grahamstown 6140, South Africa

1 Introduction

Sediment dynamics have been shown to be influenced by changes to land use and landscape connectivity in catchments worldwide (Walling 1999; Brierley et al. 2006). The upper Thina catchment is an important high rainfall water resource in the northern Eastern Cape, South Africa, and is an example of how ongoing subsistence farming on communal land is thought to have led to overgrazing and trampling that has initiated large erosive features (e.g., gullies) and river incision (van der Waal 2014). High suspended sediment loads characterise storm flow and threaten ecological and socio-economic capital (van der Waal 2014). Sediment accumulation on flood benches and floodplains takes place by laminar accrual over time; thus, sediment dating combined with sediment tracing can be used to construct a record of sediment origin to assess spatial and temporal changes in connectivity between sources and sinks (Collins et al. 1997a; Foster et al. 2011).

Sediment fingerprinting is a well-established method which has proven its value in revealing the erosion of sediment sources and downstream delivery of sediment (Walling

Published online: 06 August 2015

et al. 1979; Walling and Woodward 1995; Collins et al. 1997a, b, 2010; Foster et al. 1998, 2007; Wallbrink et al. 1998; Carter et al. 2003; Collins and Walling 2007; Manjoro 2012; Walling 2013). Sediment fingerprinting aims to identify and estimate the percentage contributions from various sources documented in the catchment. Assuming that the tracers used are conservative during sediment erosion, transport, deposition and post-depositional storage, it is possible to trace historically deposited sediment stored in depositional environments (Collins et al. 1997a; Hancock and Pietsch 2008; Rowntree et al. 2012).

Research was carried out in the Vuvu catchment, a subcatchment of the Thina River (Fig. 1). The upper and lower areas of the catchment are distinguished by geology and land use. The upper catchment is underlain by igneous rocks (basalt) and is used predominantly for grazing. The lower catchment is underlain primarily by sedimentary rocks (mudstones and, locally, sandstone) and has been used for village settlement, cultivation and grazing. This distribution of land use types within the catchment has changed little over the past 100 years, although the intensity of land use has increased within each catchment zone as the population progressively increased since the twentieth century, but possibly stabilised around the twenty-first century (van der Waal 2014). The lower catchment has been the most affected by land use change and an associated increase in hillslope–channel connectivity and thus could be a significant source of sediment (van der Waal 2014). The aims of this investigation were to determine the relative contributions of sediment from the two areas of the catchment and to see whether sediment sources and downstream sedimentation rates have changed over the past century. Radionuclide dating was used to reconstruct the sediment chronology of flood deposits to assess changes in sedimentation rates over the last 100 years. The difference in land use and geology between the upper and lower catchment was used to discriminate sediment source groups. Thus, historical changes to the relative contributions to flood deposits from the upper and lower catchment due to land use change could be inferred. This paper also investigated the potential for a simplified fingerprinting parameter employing a single sediment property to be used as a reliable qualitative tracer in this and future studies in this area. Using a single magnetic tracer would significantly reduce the future costs and time requirements in a region where resources are limited.

1.1 Study area

The Vuvu catchment (Fig. 1) (area of 65 km^2) is located in the northern Eastern Cape or former Transkei homeland, South Africa, and drains the Drakensberg Escarpment before joining the Thina River, a tributary of the Umzimvubu River. The uppermost divide of the catchment forms the border between South Africa and Lesotho. The catchment is located in the mountainous foothills of the southern Drakensberg, also known as the Great Escarpment geomorphic province (Partridge et al. 2010). The Drakensberg runs northeast to southwest with long narrow spurs extending from the escarpment, creating many ridges and plateaus separated by deep valleys (De Decker 1981; Mucina et al. 2006). The Vuvu catchment is elongated and drains from west (2920 m above sea level (asl)) to east (1450 m asl). The catchment is underlain by the Karoo Supergroup rocks comprising Drakensberg Group basalts and Clarens Formation sandstones overlying Elliot Formation mudstones. Quaternary alluvium occupies the valley bottom (Fig. 2) (De Decker 1981). Soils on the steep hillsopes are shallow and rocky lihosols with depths of around 20 cm; on gentler slopes, colluvial soils can be up to 6 m deep (maximum depth of gullies) (Fey et al. 2010). Due to the steep topography, the Vuvu system has a high-density dendritic drainage network (Fig. 1). Limited valley floor sediment storage space exists due to the steep slopes and confined nature of the valleys. A narrow valley fill occupies the lower section of the main valley.

Average annual rainfall varies from 707 to 928 mm and increases with elevation (Mucina et al. 2006), up to 2100 m asl, whereafter rainfall and rainfall intensity decrease (Nel et al. 2010). Precipitation peaks in summer, in the form of high-intensity thunderstorms (Nel 2008), with snow during winter (Mucina et al. 2006). Flow is perennial and peaks in summer. The catchment is undammed and thus has a fairly natural flow regime, with the impact of overgrazing and consequent erosion being responsible for any anthropogenic changes to the hydrology.

Grassland dominates the vegetation and varies between Lesotho Highland Basalt Grassland (1900–2900 m asl), Southern Drakensberg Highland Grassland (1720–1900 m asl), East Griqualand Grassland (920–1720 m asl) and small pockets of Mistbelt Forest in ravines (Mucina et al. 2006).

Accelerated soil erosion, through features such as gullies, soil pipes and sheet and rill erosion, is common throughout this region (Beckedahl et al. 1988; Beckedahl and Dardis 1988). The acceleration of erosion has been attributed to poor farming practices and artificial drainage (Beckedahl et al. 1988; Dardis and Beckedahl 1988). van der Waal (2014) proposed that erosional features have enhanced the hillslope–river channel connectivity over the past 50 years, potentially increasing the sediment yield from the catchment.

2 Materials and methods

2.1 Sediment source sampling

Colour digital aerial images from 2009 (1:10,000; 0.5 m resolution; acquired from Chief Directorate: National Geo-spatial Information, South Africa) were used in ArcInfo 10.0 to

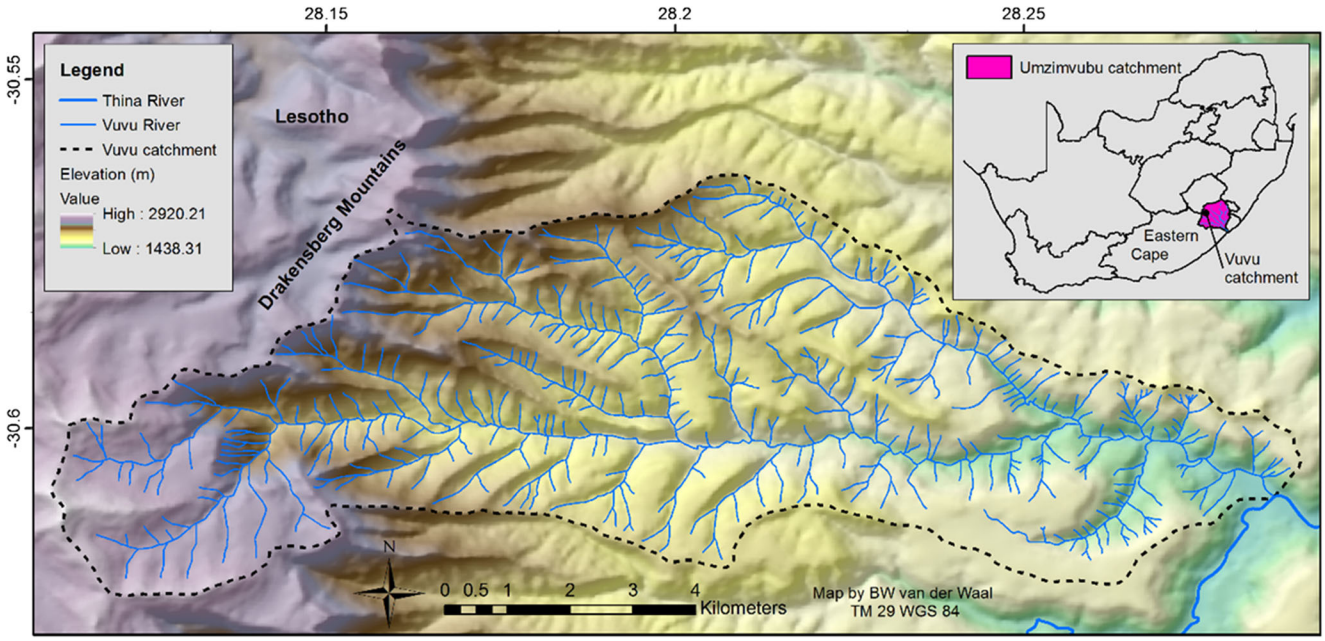

Fig. 1 The topography and drainage network of the Vuvu catchment. The location of the catchment in relation to South Africa and the Umzimvubu catchment is indicated on the *inset map*

manually digitise active hillslope sediment sources at a scale of 1:2000 for the entire Vuvu catchment. Sediment source areas were classified into three groups based on parent material, namely basalt (Drakensberg Group), sandstone (Clarens Formation) and mudstone (Elliot Formation). The main erosion features identified in each parent material group were visibly eroding and incised agricultural fields, gullies, areas of severe sheet erosion (referred to as sheet erosion) and landslides. Each of the mapped gully, sheet erosion and landslide features was converted to a point based on the centroid of the feature. All the points were lumped together and stratified random sampling was used to target 100 sampling points. Sites were apportioned by area of each geological type. The largest number was on the Drakensberg Group (49 sites), followed by the Elliot Formation (40 sites) and the Clarens Formation (11 sites). A Garmin GPSMAP device was used to navigate the sites. Seven of the sites could not be reached due to potentially dangerous and challenging terrain.

A stainless steel (non-magnetic) corer was used to collect surface samples to a depth of 10 cm. Samples were extracted near the edge of the erosion feature where there was dense grass cover. It was assumed that the grass cover was indicative

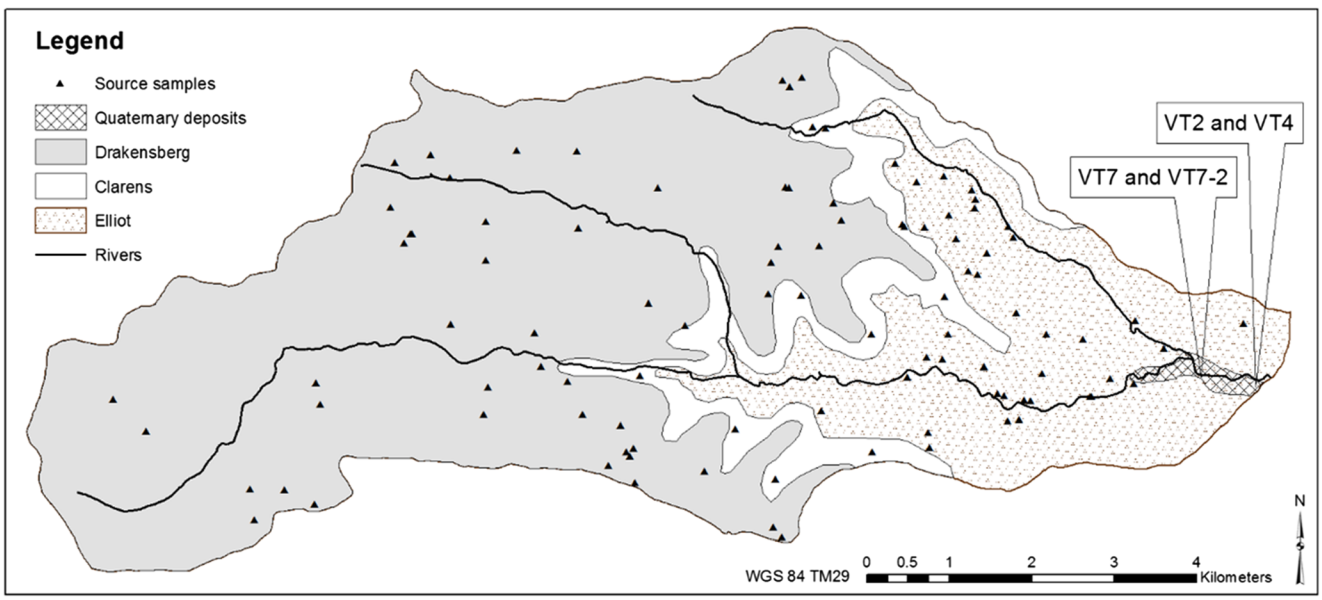

Fig. 2 The geology (De Decker 1981) of the Vuvu study area and the location of sampling sites used for source tracing and coring

of a relatively undisturbed surface soil which would represent the surface material that had been lost from the adjacent erosion feature. In addition, a horizontal sub-surface sample was taken from the middle horizons of visibly eroding gullies, sheet erosion and landslides. For large features (deeper than 1.5 m), several sub-surface samples were extracted at 1 m intervals. A total of 200 samples were taken from 93 sites: 93 surface and 107 sub-surface.

2.2 Historically deposited sediment sampling

The valley floor alluvial morphology consisted of terraces and two levels of flood benches. Flood benches represent the most recent sediment sink in the valley fill. Field evidence (e.g., debris and fine sand deposits on the higher benches and fresh deposits of up to 4 cm of sand on the lower benches after the 2012/2013 wet season) indicated that both levels are still active depositional environments.

Cores were taken from flood benches using an Eijkelkamp percussion corer (nose diameter 4.5 cm) (Eijkelkamp, The Netherlands). Four cores were positioned to target two higher flood benches (VT2 and VT7-2, inundated less frequently) and two lower flood benches (VT4 and VT7, inundated relatively frequently) (Fig. 3). Their location was spread along the lower reach of the valley fill (VT2, VT4; VT7, VT7-2; Fig. 2). Care was taken to core undisturbed locations where horizontal sediment layering was clearly visible throughout the sequence. All cores were taken from the upper sandy sequence until a cobble layer was encountered (often visible in the bank). The cores ranged between 60 and 120 cm length and were cut into 2 cm slices (i.e., 30 to 60 samples per core).

2.3 Laboratory methods

Samples were oven dried for 48 h at 40 °C (Yu and Oldfield 1989) to preserve magnetic characteristics. Median particle size and organic content were determined using a Malvern Mastersizer 3000 laser granulometer (Malvern, UK) and loss on ignition (LOI) in a muffle furnace at 450 °C, respectively. The particle size of the flood bench deposits was determined to be primarily (>85 %) in the <250-μm fraction. Both source and core samples were therefore sieved to this particle size to reduce errors in the tracers (Collins et al. 1997a; Walling 2013).

Mineral magnetic signatures were used as tracers for sediment sources as they have previously shown potential to discriminate between igneous and sedimentary rock formations (Dearing 1999; Oldfield 1999; Rowntree and Foster 2012). Although magnetic signatures have been shown not to be perfectly linearly additive, errors caused by non-linear additivity have been shown to be small (Lees 1997). Mass-specific

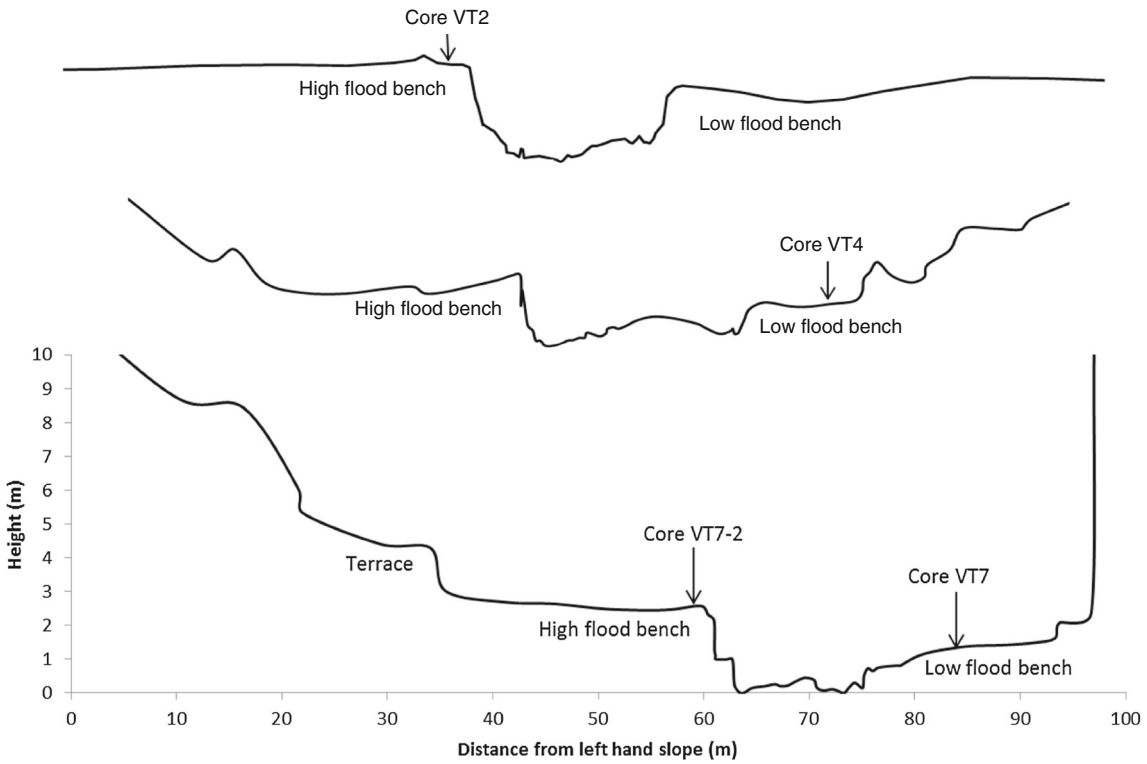

Fig. 3 Transects VT2, VT4 and VT7 indicating the location of cores VT2, VT4, VT7 and VT7-2. The *horizontal* and *vertical scales* are identical for all transects

magnetic susceptibility and remanence properties were determined for 5–10 g of <250 μm sediment packed into 10 ml pots. The Bartington® susceptibility meter (Witney, UK) with an MS2B dual frequency sensor was used to measure high- and low-frequency magnetic susceptibility (Maher 1986; Dearing 1999). The susceptibility readings were corrected for the organic content using the LOI data and expressed as minerogenic low (Xlf) and high (Xhf) frequency magnetic susceptibility (Foster et al. 1998). The remanence properties as explained by Walden (1999) and Foster et al. (2008)—anhysteretic susceptibility (XARM ($ARM_{40\ \mu T}\times 3.14\times 10$), isothermal saturation remanence ($SIRM_{1\ T}$), hard isothermal remanence (HIRM ($SIRM_{1\ T}/(1-(-1\times(IRM_{100\ mT}/SIRM_{1\ T})))/2$)—were measured using the Molspin® rotating magnetometer, Molspin® a.f. demagnetiser and a Molspin® pulse magnetiser using the methods laid out by Maher (1986), Walden (1999) and Foster et al. (2007).

The radionuclides ^{137}Cs, ^{214}Pb and total ^{210}Pb were detected using an Ortec gamma spectrometer (Oak Ridge, USA). PTFE sample containers were filled with the <250-μm sediment to the well depth (4 cm) of the hyper pure germanium crystal in the spectrometer. Samples were sealed with paraffin wax and left to equilibrate for 21 days before being counted (Foster et al. 2007). A background spectrum was generated by counting an empty vial for >10,000 s. The background was stripped from counted spectra and the resultant spectra were analysed using GammaVision® software. Emissions were counted for >180,000 s to allow for the detection of low radionuclide activity at the 95 % level of confidence. Detectible limits for ^{137}Cs, ^{214}Pb and total ^{210}Pb were 0.8, 2.2 and 2.5 mBq g^{-1}, respectively.

Caesium-137 was used to indicate surface soil contributions in sediment cores and to assess the extent of surface soil loss since 1958. A selection of surface samples (n=28) was analysed for the presence of ^{137}Cs attached to <250 μm particles. ^{137}Cs fallout is assumed to be spatially homogeneous at a relatively small scale (Walling 2004, 2005). Absence of ^{137}Cs in the surface soil would therefore indicate that the top soil horizon (upper 10 cm) has been totally eroded since 1958. ^{137}Cs in the core samples can also be used to indicate proportions of sediment originating from surface soils which were eroded after the first detectable ^{137}Cs fallout in 1958 (Foster 2006). ^{137}Cs could not be used as an indicator of surface soil contributions for portions of the core that dated between 1955 and 1975 as sediment was potentially ^{137}Cs labelled by direct fallout. ^{137}Cs activities in surface samples were not used to calculate rates of soil erosion for reasons discussed by Parsons and Foster (2011) and the absence of a non-eroded site to obtain a reference inventory. Additionally, the abundance of rocky outcrops in this study catchment would result in an initial non-uniform distribution of ^{137}Cs in topsoils. As ^{137}Cs is not always detectable in topsoil, non-^{137}Cs-bearing soil is being exported from the slope, which soil erosion models based on fallout radionuclides cannot account for.

2.4 ^{210}Pb and ^{137}Cs dating

Unsupported ^{210}Pb in combination with ^{137}Cs was used to date the more recent flood benches (Saxena et al. 2002; Saint-Laurent et al. 2010; Du and Walling 2012), and historical aerial images were used to verify flood bench dating. ^{137}Cs appeared in the Southern Hemisphere around 1958 (Foster et al. 2007). ^{137}Cs can thus be used as a marker horizon since all sediment containing ^{137}Cs has been deposited post-1958 (Foster et al. 2005).

Unsupported ^{210}Pb was first used for dating sediments from lake environments, but recently, the method was successfully applied to floodplain environments using the constant rate of supply (CRS) model (Saint-Laurent et al. 2010; Du and Walling 2012; Manjoro 2012). As floodplain sediment is not constantly inundated by water and the sediment calibre is likely to be greater than that of lake sediments, a proportion of the ^{222}Rn is expected to escape from the sediment. An emanation coefficient of 0.3, which resulted in positive unsupported ^{210}Pb values, was used to adjust the supported ^{210}Pb values in order to compensate for the loss of ^{222}Rn (the mother isotope). This value is also recommended by Du and Walling (2012). The unsupported ^{210}Pb was calculated by subtracting the supported ^{210}Pb from the total ^{210}Pb. This result was used in the composite CRS model, as this model has been proven to be reliable in areas with varying sedimentation rates, especially if ^{137}Cs is used to adjust the CRS age (Appleby 2001; Du and Walling 2012).

Historical aerial images were used to verify the ^{137}Cs marker horizons. Aerial images for 1956, 1966 and 1975 were georeferenced to georectified aerial images for 2009. The active channel along the Vuvu valley fill was digitised for each set of images. Photos were assessed from the most recent to the oldest date. If the core location was in the channel in an aerial image, the date of the bottom of the core was adjusted to the date of the image, assuming that sediment deposition at the core location started soon after the date of the photo.

A shortcoming noted by Appleby (2008) is that in areas with rapid sediment accumulation, ^{210}Pb activities are diluted and could limit the dating horizon to three to four half-lives (e.g., 66–88 years) instead of six half-lives if the surface (peak) activity is lower than 100 mBq g^{-1}. In the Vuvu catchment, peak counts were in the region of 60 mBq g^{-1} so dating was limited to a maximum of 88 years.

2.5 Sediment source tracing

Quantitative sediment source fingerprinting was used on the most complete core (VT2). The approach was based on the work of Lees (1994) and Collins et al. (1997b), which has two main protocols: (1) test if tracers can distinguish between the source groups and select the optimum set of fingerprint properties and (2) apportion the contributions from each source group using a multivariate unmixing model. The outcome of the sediment source fingerprinting was compared to the predictions of a single tracer, with the aim of simplifying sediment source tracing for this and future research.

A mass conservation test was performed on each tracer by determining if the magnetic signatures of the sediment fell within the range of the mean plus or minus one standard deviation of the source groups (Collins et al. 1997b). If a magnetic signature of the sediment fell outside of the range found in the source samples, it would indicate that a potential source was missed during sampling or that the tracer signatures changed during transport or after deposition; these signatures were therefore removed from further analysis.

The tracer signatures of the source samples were interrogated statistically to test if the magnetic signatures could discriminate between the sediment source groups. The null hypothesis, that there was no significant difference for tracers between the various geological zones, was tested using the two-tailed Kruskal-Wallis *H* test.

Tracers that passed the mass conservation test and the Kruskal-Wallis test were used in a stepwise discriminant function analysis (DFA) to identify the composite fingerprint of tracers able to best differentiate between the source groups (Collins et al. 1997b; Foster et al. 2007). The composite fingerprint of tracers that correctly classified the highest percentage of source samples into their respective groups was used in a multivariate mixing model which incorporated the Monte Carlo uncertainty analysis based on 3000 random iterations per sample from within the mean±1 standard deviation of each source group (Collins and Walling 2007). A probability density function was produced by the unmixing model (Eq. (Appleby 2001)) from which the proportional contribution of sediment from each source group and associated uncertainty were extracted:

$$\sum_{i=1}^{n}\left\{\left(C_i-\left(\sum_{s=1}^{m}P_sS_{si}\right)\right)/C_i\right\}^2 \quad (1)$$

where C_i = the concentration of fingerprint property in the sediment sample, P_s = the optimised percentage contribution from the source category, S_{si} = the median concentration of fingerprint property in the source category, n = the number of fingerprint properties comprising the optimum composite fingerprint and m = the number of sediment source categories (Collins et al. 2010). No weightings or correction for particle size was applied as it is likely to introduce unquantified error (Smith and Blake 2014).

Goodness of fit (GOF) was calculated to define the difference between actual and modelled values using

$$\mathrm{GOF}=\left\{1-\left(C_i-\left(\sum_{s=1}^{m}P_sS_{si}\right)\right)/C_i\right\}*100 \quad (2)$$

The results of the quantitative tracing results for core VT2 were compared to the low-frequency magnetic susceptibility (Xlf) of the sediment (using regression analysis) to determine if Xlf was sufficient alone to apportion contributions from the two geological areas. Xlf was used on the basis that it measures the response of all magnetic grain types in a sample to an externally applied magnetic field and, therefore, integrates the other magnetic measurements which measure specific grain types.

3 Results

3.1 Erosion of the various source areas

The largest part (65 %) of the Vuvu study site (58 km^2) is underlain by the Drakensberg Group lithology, followed by the Elliot (25 %) and Clarens (10 %) Formations. Of the erosion features (gully erosion, sheet erosion and landslides) that were visually assessed in the field (n=78), 63 % were judged to be still actively eroding (floor and sidewalls actively eroding; Table 1). The remaining 38 % showed signs of floor stabilisation with bottoms being colonised by vegetation, although sidewalls were still actively eroding. It is evident that a large proportion (61–83 %) of gullies are still eroding, whereas the majority (79–86 %) of areas with sheet erosion have stabilised (Table 1).

Caesium-137 was used as an indicator for surface soil loss, as its activity is likely to reflect the degree of erosion (Bajracharya et al. 1998). ^{137}Cs data for surface samples suggested that half of the catchment's surface soils had lost the

Table 1 Summary of erosion features visited during source sampling. Percentages indicate the proportions of stable or unstable features. Sample size is given in brackets

Geology	Feature	% Stable	% Unstable
Drakensberg	Gully (n=16)	37.5	62.5
	Sheet (n=21)	85.7	14.3
Clarens	Gully (n=6)	16.7	83.3
	Sheet (n=1)	0.0	100.0
Elliot	Gully (n=18)	38.9	61.1
	Sheet (n=14)	78.6	21.4
	Landslide (n=2)	50.0	50.0

entire top layer containing ^{137}Cs since 1958 (Table 2). When considering individual geological zones, ^{137}Cs was present in both Clarens Formation topsoil samples, indicating low erosion rates for this small sample, while the Elliot Formation and the Drakensberg Group have lost all ^{137}Cs from 63 and 40 %, respectively, of their topsoil samples. Although the per cent of 'eroded' soils is lower, the eroded area of the Drakensberg Formation is 61 % greater than that of the Elliot formation, so the potential soil loss is significant.

3.2 Core samples and sediment chronology

Median particle size (D_{50}) for the core samples ranged between 58 and 343 μm (coarse silt to medium sand). ^{137}Cs activities in the cores ranged between 0 and 4.3 mBq g^{-1}, with multiple peaks throughout each of the down-core profiles, except VT7-2 which had a single peak (Fig. 4A). All cores except VT4 had a section with no detectable ^{137}Cs at the bottom of each core. The first detection of ^{137}Cs from the base of the core can thus be used as the 1958 marker, assuming that no down-core migration of the tail has taken place.

Historical aerial images challenged the use of ^{137}Cs as an absolute marker as the locations of cores VT4 and VT7 were situated in the channel on the 1956 images. The flood bench had started forming in the position of VT7 by the time of the 1966 images. This suggests either rapid sediment accumulation before the 1958 ^{137}Cs marker or low ^{137}Cs activity of the lower section of the core due to the coarse nature of the sediment, possibly sourced from sub-surface sources. The date of the base of core VT7 was adjusted to fit the aerial image date of 1956; the composite CRS model had dated it to 1920. Likewise, on the 1966 aerial photos, the location of core VT4 was situated in the active channel, but outside the channel in the 1977. This would agree with the ^{137}Cs found near the bottom of the core, but the first occurrence of ^{137}Cs could not be used as a 1958 marker and the bottom of core VT4 was adjusted to 1966.

Unsupported ^{210}Pb values increased towards the surface for the higher lying cores, VT2 and VT7-2. This showed that sediment has been accumulating at a steady rate at these higher sites, whereas the lower level cores—VT4 and VT7—showed large variation in values with minimal unsupported ^{210}Pb accumulation towards the top, suggesting rapid sediment accumulation. The dates produced for the higher lying cores estimated the initiation of accumulation as pre-1920 (Fig. 4B). The chronologies that were produced for all cores were in agreement with the historical images that were assessed.

Sediment accumulation rates (SAR) based on the composite CRS model varied between 0.2 and 3.3 g cm^{-2} year^{-1} for the higher flood benches and 0.6 and 11 g cm^{-2} year^{-1} for the lower flood benches. This is in agreement with the infrequent inundation of the higher benches compared to the lower benches.

Table 2 The presence of ^{137}Cs in surface soil samples

	Number	^{137}Cs present	% with no remaining ^{137}Cs
All	28	14	50
Drakensberg	10	6	40
Clarens	2	2	0
Elliot	16	6	63

3.3 Tracing

The null hypothesis, that there was no significant difference between the geological zones, was rejected for all tracers used; at least one parent material grouping was significantly different from the other groups in the Kruskal-Wallis H test (Table 3). The largest difference is between the Xlf values of the source groups (H=142). Further expansion of these results, using multiple comparisons, showed that the largest differences were present between the igneous Drakensberg Group and sedimentary Clarens/Elliot Formations (Table 3). Average magnetic signatures and D_{50} were larger for the Drakensberg Group compared to the sedimentary rock sources. There were no significant differences between tracer concentrations in the Clarens and Elliot Formations. For this reason, they were combined into a single source group for the remainder of the analysis. The two groups will be referred to hereafter as igneous and sedimentary sources, referring to the rock types forming the soil parent material.

All tracer values in the cores fell within the source values, thus passing the mass conservation test and allowing for their continued use in the source tracing (Table 4). Results from the DFA showed that the best igneous and sedimentary source discrimination was achieved using a composite fingerprint consisting of Xlf, ARM and HIRM and classified 96 % of source samples correctly into their respective groups. Using these tracers in the unmixing model resulted in an apportionment result for core VT2 that was dominated by sedimentary sources (Elliot and Clarens Formations) throughout most of the core (Fig. 5A). Sedimentary sources contributed on average 64 % of the sediment, with the remainder (36 %) signified by igneous sources. Mean uncertainty for the contributions was 10 % with error margins ranging between 3 and 27 %. The average goodness of fit (agreement between optimised mixing model results and measured fingerprint property) for the apportionment was 87 %.

The negative relationship between GOF and D_{50} indicated that apportionment accuracy decreases with an increase in particle size (R^2=0.64) (Fig. 6A). Results of sediment tracing for coarser layers should thus be interpreted with caution and in the light of the particle size range for the various sources. Particle size was however determined not to be the primary

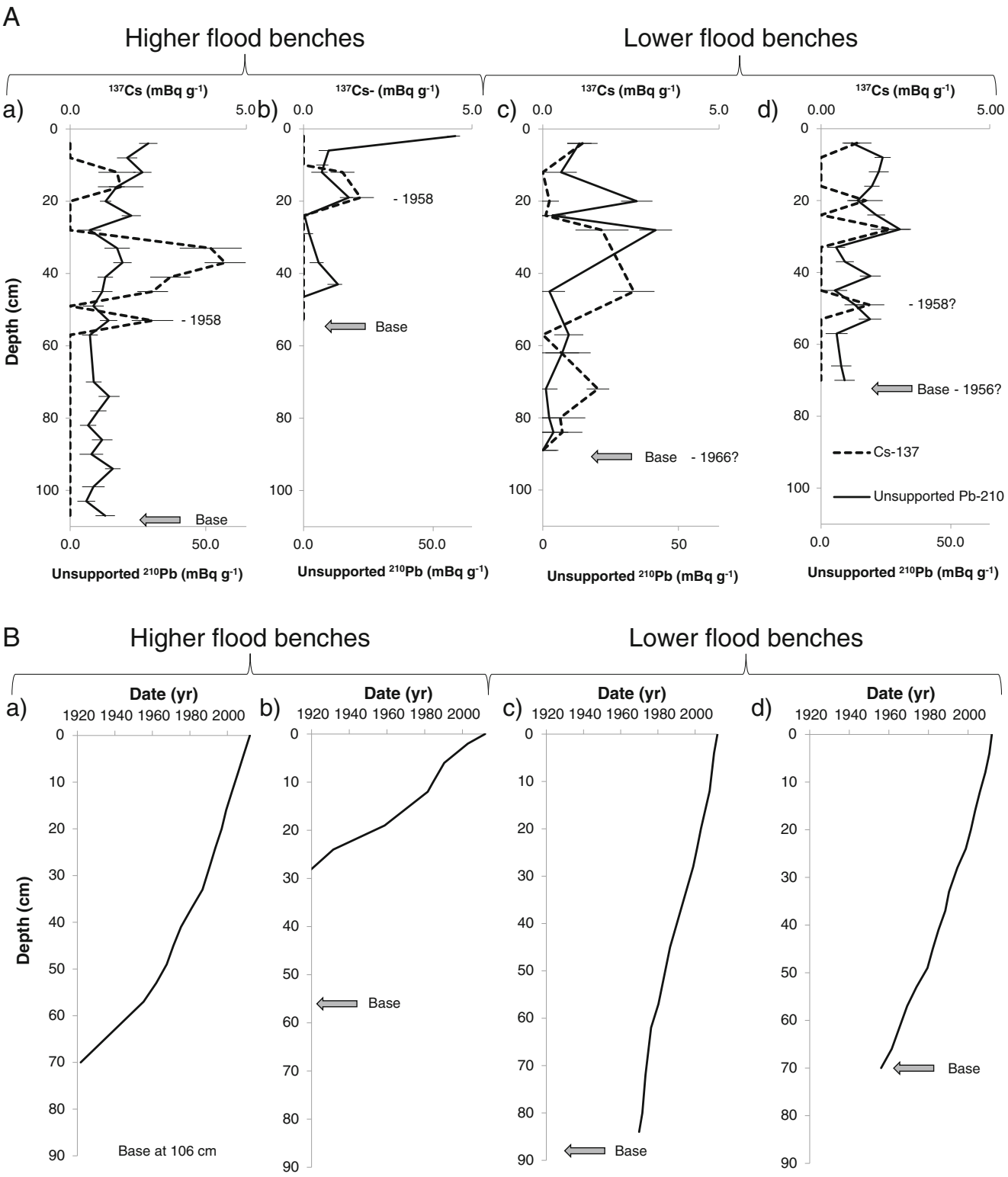

Fig. 4 **A** ^{137}Cs and unsupported ^{210}Pb data for the cores: *a* VT2, *b* VT7-2, *c* VT4 and *d* VT7. **B** CRS dates for cores *a* VT2, *b* VT7-2, *c* VT4 and *d* VT7

control for the magnetic signature (R^2=0.08) (Fig. A1, Electronic supplementary material).

The potential for Xlf to act as a sole tracer was also assessed for core VT2. The median Xlf values of sedimentary (0.4×10^{-6} m^3 kg^{-1}) and igneous sources (5.1×10^{-6} m^3 kg^{-1}) (Fig. 5B) showed large differences between the two source groups with minimal overlap between values. From the Xlf values of core VT2, it can be seen that the sediment was a mixture from both source groups (Fig. 5). The Xlf values tended to be nearer to the sedimentary source range, indicating

Table 3 Kruskal-Wallis *H* test and multiple comparisons for magnetic signatures and median particle size (D_{50}) for samples from the various parent materials. Mean values and standard deviation (SD) are given for the variables

Variable	*H* (*n*=193)	*df*	*p*	Drakensberg-Clarens	Drakensberg-Elliot	Clarens-Elliot	Drakensberg		Clarens		Elliot	
							Mean	SD	Mean	SD	Mean	SD
Xlf	141.9	2	*0.000*	*0.000*	*0.000*	0.233	5.4	2.1	0.8	0.4	0.4	0.3
SIRM	140.4	2	*0.000*	*0.000*	*0.000*	0.482	121.4	64.2	7.0	3.4	4.7	2.8
IRM	136.1	2	*0.000*	*0.000*	*0.000*	0.484	70.7	40.4	3.9	2.7	2.2	1.9
XARM	134.5	2	*0.000*	*0.000*	*0.000*	0.619	48.0	25.6	7.4	3.9	5.3	7.7
ARM	134.5	2	*0.000*	*0.000*	*0.000*	0.619	1.5	0.8	0.2	0.1	0.2	0.2
HIRM	129.1	2	*0.000*	*0.000*	*0.000*	1.000	15.5	9.9	1.3	0.4	1.1	0.5
Xfd	96.9	2	*0.000*	*0.006*	*0.000*	0.123	237.6	172.6	82.0	45.7	46.0	35.6
D_{50}	18.4	2	*0.000*	0.775	*0.000*	0.807	93.5	53.4	66.5	20.9	60.0	22.2

Significant *p* values are italicised

that the majority of the sediment was of sedimentary origin, with layers that have a larger igneous input.

Figure 5 demonstrates that the sediment provenance predictions follow a very similar trend for both the quantitative and qualitative sediment tracing of core VT2. The quantitative approach produces estimated proportions with the amount of error related to the apportionment, whereas the qualitative approach gives an indication of an increased or decreased contribution from a specific source without an error estimate. The agreement between the two approaches is confirmed by the strong positive relationship (R^2=0.95) between the percentage contribution from the igneous source and Xlf (Fig. 6B):

$$y = 32.077\ln(x) + 12.402 \quad (3)$$

where x is Xlf (10^{-6} m^3 kg^{-1}) and y is the percent contribution from an igneous source.

Equation (3) can thus be used to calculate the contribution from an igneous source based on the Xlf value of the sediment. The equation would enable sediment source tracing for other stored sediment and future monitoring based on Xlf values alone. A sediment Xlf value of 3×10^{-6} m^3 kg^{-1} defines equal contributions of igneous and sedimentary sources (Fig. 6B). This benchmark, in combination with Eq. (3), was used to interpret further sediment tracing where the aim was to see if there was a shift in sediment source over time (Fig. 7).

Xlf was used on its own to examine down-core contributions from igneous and sedimentary sources in all four flood benches (Fig. 7). It can be seen that the relative contribution from the two sources varied over time, but there was no clear trend indicative of a definite shift in sediment source over the past 50–100 years (Fig. 7).

Source contributions varied between the cores as can be seen in Fig. 7. Cores on the higher flood benches had igneous contributions ranging from 22 to 59 % (Xlf of 1.3–4.3 × 10^{-6} m^3 kg^{-1}), indicating a mixture of sources that were mainly sedimentary but with greater igneous contribution during defined periods, as can be seen for VT2 from 55 to 77 cm (Fig. 7). Sediment on the lower flood benches had a greater contribution from sedimentary parent materials than the higher benches (range of igneous contribution 3–50 %). In the flood bench cores, sediment derived from igneous sources had the greatest ^{137}Cs activity, whereas layers without ^{137}Cs were often from a sedimentary source. This would suggest that igneous material had a greater topsoil component, while sedimentary source material came from subsoils.

Table 4 Summary of the mass conservation test results

Tracer	Source parent lithology				Core	
	Igneous		Sedimentary		Sediment	
	Mean	SD	Mean	SD	Mean	SD
Xlf[a]	5.4	2.1	0.5	0.3	1.8	0.9
Xfd[a]	237.6	172.6	50.7	38.8	57.8	49.9
ARM[a]	1.5	0.8	0.2	0.2	0.5	0.7
XARM[a]	48.0	25.6	5.6	7.4	14.8	20.6
SIRM[a]	121.4	64.2	5.0	2.9	50.0	32.9
$IRM_{100\ mT}$[a]	70.7	40.4	2.4	2.1	29.9	19.8
HIRM[a]	15.5	9.9	1.1	0.5	8.8	6.0

[a] Indicates that the signature passed the test

4 Discussion

The emanation coefficient of 0.3, as used by Du and Walling (2012), made the use of the composite CRS method possible in the flood benches. A combination of ^{137}Cs and historical aerial photos was used to calibrate the age of the model.

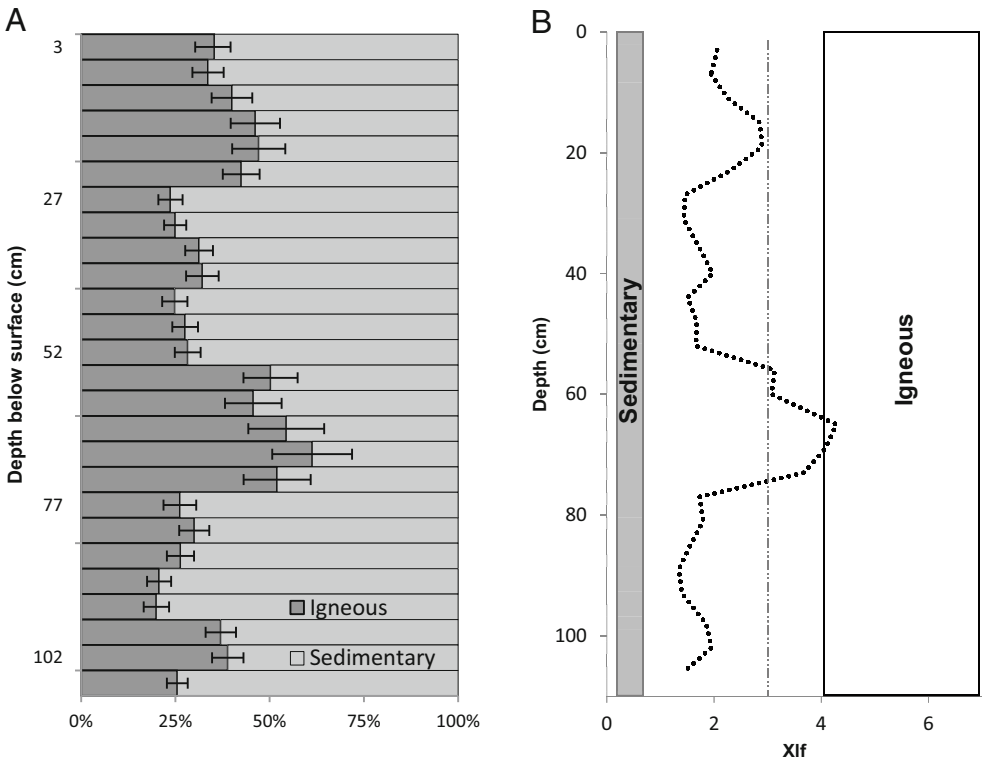

Fig. 5 Sediment apportionment for VT2 showing **A** quantitative output including standard deviation *error bars* and **B** Xlf values for VT2. *Boxes* are used to indicate the Xlf quartiles (25–75 %) for sedimentary and igneous source samples

Conditions for using the method were not ideal as the ^{137}Cs activity was relatively low, as would be expected for the Southern Hemisphere (Foster et al. 2007). The use of photos proved invaluable for cores VT4 and VT7. If the model was only based on the first occurrence of ^{137}Cs from the base upwards, the dating at the bottom of the cores VT4 and VT7 would have been inaccurate by more than 8 and 36, respectively. The calibration date for that slice was changed from 1958 (based on the first occurrence of ^{137}Cs) to 1966+, as the slice below the ^{137}Cs marker slice was given the date 1966 based on historical aerial images. Similarly, for VT7, where the 1958 marker was two thirds down the core, the date for the base was calculated from the model as 1920. Aerial images proved that the date for the base of the core VT7 was closer to ~1956. This shows the importance of additional evidence such as historical aerial images when using ^{210}Pb and ^{137}Cs to date flood benches.

The dates derived from the composite CRS model showed temporally variable sediment accumulation rates, as would be expected for flood benches with varying degrees of channel flood bench connectivity over time. Unsupported ^{210}Pb activities for the higher flood benches increased towards the top of the sequence as was to be expected for undisturbed sediment chronologies that accumulated at a steady rate. The greater fluctuation in unsupported ^{210}Pb values for the lower flood benches shows periodically rapid accumulation of sediment as was expected due to more frequent channel–flood bench connectivity.

The sediment sequences on the higher flood benches were estimated to be >92 years old compared to the lower flood

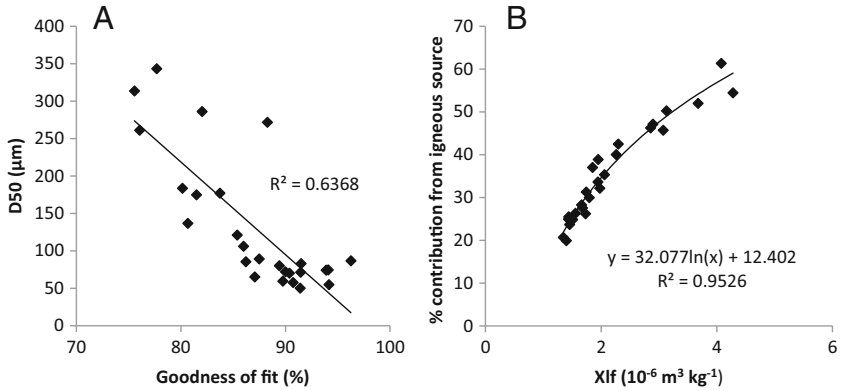

Fig. 6 Apportionment results: **A** the relationship between median particle size and goodness of fit and **B** the relationship between Xlf and the contribution of igneous material

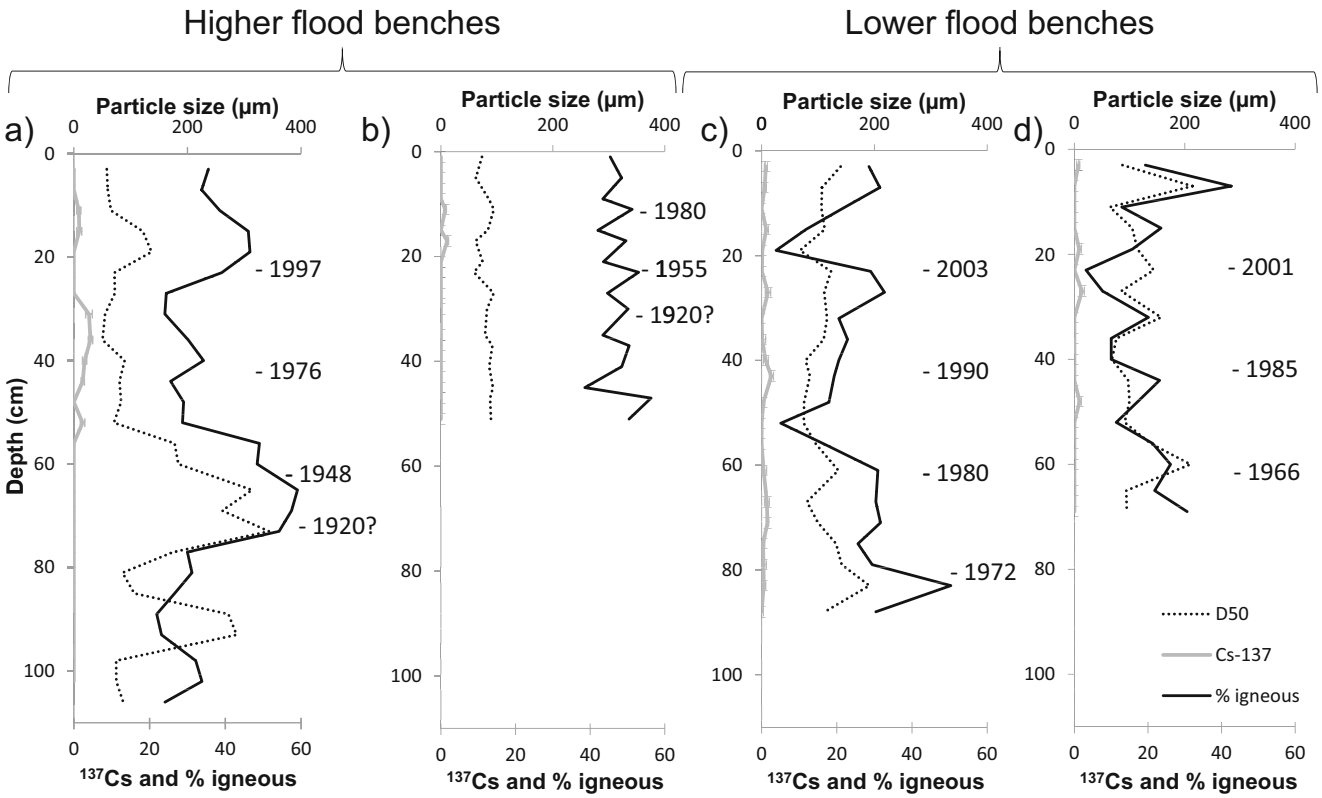

Fig. 7 Down core median particle size, ^{137}Cs activity (mBq g^{-1}) and percent contribution from igneous sources for cores *a* VT2, *b* VT7-2, *c* VT4 and *d* VT7

benches which were estimated to be 46–60 years old. The higher lying flood bench VT7-2 showed low accumulation rates that reflected infrequent channel–flood bench connectivity. An increase in SAR for the higher level cores since 1958 was unexpected as channel–flood bench connectivity usually becomes less frequent as a flood bench is built up vertically. If this increased SAR over the last 50 years is real, it points to either an increased channel–flood bench connectivity due to increased storm flow and/or to high sediment loads due to increased catchment erosion.

Sedimentation trends also varied for the lower flood benches, with an overall increase in SAR as the lower flood benches were built up, again indicating an increase in channel–flood bench connectivity and sediment deposition. The results for both sets of flood benches support the observations that were made in the field of an increasingly connected and degraded catchment (Table 1).

The SAR post-1958 differed between the lower and higher flood benches. The average SAR for higher flood benches was 0.9 g cm^{-2} year^{-1} compared to 3.2 g cm^{-2} year^{-1} for the lower benches, reflecting the greater inundation frequency of lower flood benches (Erskine and Livingstone 1999). Evidence from aerial photographs and bank stratigraphy indicates that the lower benches are ±50 years old, coincident with incision of the main channel (van der Waal 2014). Prior to incision, the lower section of the high terraces would have been equivalent to the present lower benches, with a similar inundation frequency. Yet the SAR for the high benches is higher post-1950. This indicates significantly higher sediment loads post-1950 and is in agreement with the formation of erosional features (e.g., sheet erosion, gullies) and increased pathways (e.g., gullies, livestock tracks) in the catchment over the past 50 years (van der Waal 2014).

The results of the apportionment for the oldest and most complete core (VT2) on a higher flood bench indicated that sources overlying sedimentary lithology were dominant (64 %), with only one section where sediment contribution was equal between igneous and sedimentary sources. No linear trend of one source replacing another through time was observed, indicating that the relative contributions from the upper and lower catchment had stayed the same through the period of record.

Magnetic susceptibility (Xlf) stood out as the main discriminator between igneous and sedimentary sources. Mzobe (2014) found similar results and ascribed it to the dominance of iron-containing minerals in basalt compared to the very low iron concentration in sedimentary sources.

All four floodplain cores showed that 20–40 % of the sediment originated from igneous sources, and there was no significant trend of increasing or decreasing igneous contributions over time. There were, however, differences in small-scale changes in the sediment provenance predicted for each of the cores. This could be explained by changes in sediment provenance during the individual stages of a flood event and related flood bench inundation as was shown for this catchment (van der Waal 2014). Alternatively, differences in

sediment particle size or post-depositional changes to magnetic tracer signatures could have resulted in these differences (D'Haen et al. 2012).

Using a single tracer (i.e., Xlf) proved a practical option for further tracing in the Vuvu catchment. Using the quantitative model and Xlf alone resulted in closely matched trends in the data (R^2=0.95); both showed that sedimentary sources were dominating core VT2 with an increase in igneous material in the same section of the core. The strong correlation between the two approaches indicates that the more complex quantitative approach confirms the results of the simpler qualitative results. Comparing the two methods allowed for an equation to be developed that could estimate the percentage igneous contribution based on a single Xlf measurement (Eq. (3)). Furthermore, the relation produced a single Xlf benchmark, 3×10^{-6} m^3 kg^{-1}, that indicates equal contributions from both sources. Having a single reference point further aids the process of rapid source ascriptions.

Particle size played a role in the accuracy of the sediment tracing. Lenses with larger particles produced poorer model GOF. This is a function of a much larger range measured for magnetic tracers from igneous sources and their inherent larger particle size. Coarser sediment deposited during larger floods might thus be expected to have a larger igneous contribution. From the cores, this trend was not evident as the generally finer material on the higher flood benches had a greater igneous contribution compared to the generally coarser material on the lower flood benches that had a greater sedimentary input. This confirms that particle size was not the primary control on magnetic signature.

Although underlying only 35 % of the catchment, the tracing results point to the local sedimentary sources (mudstones and sandstones in the lower catchment) being the dominant sediment source over the past century. Additional evidence for widespread soil loss from the lower catchment was provided by the low frequency of ^{137}Cs detection in surface soils underlain by sedimentary lithologies. High erosion rates can be attributed to the high settlement density, widespread former cultivation and increased gully erosion in the lower catchment (van der Waal 2014), coupled with the high natural erodibility of the soils.

The tracing results also suggest that either igneous-derived soil is less erodible, requiring larger events for it to be mobilised, or igneous-derived sediment is stored temporarily in the upper catchment, only being transported to the lower catchment during the larger events. Evidence for the latter process is provided by the greater igneous contribution to the higher flood benches.

5 Conclusions

The composite CRS method proved successful for dating the flood benches. Historical aerial images were invaluable for the interpretation of ^{137}Cs marker horizons that were used to calibrate the composite CRS model. This suggests that when the composite CRS model is used to date flood benches in the Vuvu catchment and comparable catchments elsewhere, dates older than the 1958 ^{137}Cs marker should be used with caution and preferably be verified by field or photographic evidence.

A semi-quantitative tracing approach was developed based on Xlf values and a regression equation. This semi-quantitative approach was useful for further monitoring as source dominance can be based on a single magnetic measurement using a Bartington® susceptibility meter with an MS2B dual core sensor. It was determined that sediment source tracing can be performed in the Vuvu catchment in a semi-quantitative way using Xlf values as a tracer. This simplifies any further tracing without compromising the results.

Sediment stored in flood benches was mainly from sedimentary sources over the past century. Higher flood benches stored finer sediment with a larger input from distal sources, whereas the lower flood benches stored coarser sediment from local sources. This interaction was attributed to the dynamic nature of longitudinal and lateral connectivity as sediment from distal sources was only transported, and the channel was only connected to the higher flood bench, during the larger flow events. The lower flood bench was inundated during both large and smaller events, but sediment deposits were associated with the smaller flow events mobilising and storing locally sourced sediment.

Land use changes, especially in the lower catchment, were not observed to alter the ratio of sediment from the upper and lower catchment over the past century, thus illustrating the erodible nature of the predominantly Elliot Formation mudstones regardless of land use. It is likely that the volumes of sediment exported from the catchment have increased, due to the observed land degradation, but the lower catchment remains the dominant sediment source despite its smaller area. This reflects the sensitivity of the mudstones to land use pressures and its inherent erodible nature.

Acknowledgments We would like to thank the Water Research Commission of South Africa and the Natural Resource Management Programme of the Department of Environmental Affairs of South Africa for funding.

References

Appleby PG (2001) Chronostratigraphic techniques in recent sediments. In: Last WM, Smol JP (eds) Tracking environmental change using lake sediments. Kluwer, Dordrecht, pp 171–203

Appleby PG (2008) Three decades of dating recent sediments by fallout radionuclides: a review. The Holocene 18:83–93

Bajracharya RM, Lal R, Kimble JM (1998) Use of radioactive fallout Cesium-137 to estimate soil erosion on three farms in west central Ohio. Soil Sci 163:133–142

Beckedahl H, Dardis G (1988) The role of artificial drainage in the development of soil pipes and gullies: some examples from Transkei, Southern Africa. In: Dardis G, Moon BP (eds) Geomorphological studies in Southern Africa. AA Balkema, Rotterdam, pp 229–245

Beckedahl H, Bowyer-Bower T, Dardis G, Hanvey P (1988) Geomorphic effects of soil erosion. In: Moon BP, Dardis G (eds) The geomorphology of Southern Africa. Southern Book, Johannesburg, pp 249–276

Brierley G, Fryirs K, Jain V (2006) Landscape connectivity: the geographic basis of geomorphic applications. Area 38:165–174

Carter J, Owens PN, Walling DE, Leeks GJL (2003) Fingerprinting suspended sediment sources in a large urban river system. Sci Total Environ 314–316:513–534

Collins AL, Walling DE (2007) Sources of fine sediment recovered from the channel bed of lowland groundwater-fed catchments in the UK. Geomorphol 88:120–138

Collins AL, Walling DE, Leeks GJL (1997a) Use of the geochemical record preserved in floodplain deposits to reconstruct recent changes in river basin sediment sources. Geomorphol 19:151–167

Collins AL, Walling DE, Leeks GJL (1997b) Source type ascription for fluvial suspended sediment based on a quantitative composite fingerprinting technique. Catena 29:1–27

Collins AL, Walling DE, Stroud RW, Robson M, Peet LM (2010) Assessing damaged road verges as a suspended sediment source in the Hampshire Avon catchment, southern United Kingdom. Hydrol Process 24:1106–1122

D'Haen K, Verstraeten G, Degryse P (2012) Fingerprinting historical fluvial sediment fluxes. Prog Phys Geog 36:154–186

Dardis G, Beckedahl H (1988) Drainage evolution in an ephemeral soil pipe-gully system, Transkei, Southern Africa. In: Dardis G, Moon BP (eds) Geomorphological studies in Southern Africa. AA Balkema, Rotterdam, pp 247–265

De Decker R (1981) Geology of the Kokstad area (sheet 3028). Geological survey, Government printer, Pretoria

Dearing J (1999) Magnetic susceptibility. In: Walden J, Oldfield F, Smith J (eds) Environmental magnetism: a practical guide. Quaternary Research Association, London, pp 35–62

Du P, Walling DE (2012) Using ^{210}Pb measurements to estimate sedimentation rates on river floodplains. J Environ Radioactiv 103:59–75

Erskine WD, Livingstone E (1999) In-channel benches: the role of floods in their formation and destruction on bedrock confined rivers. In: Miller AJ, Gupta A (eds) Varieties of fluvial form. Wiley, New York, pp 445–475

Fey M, Hughes J, Lambrechts J, Dohse T (2010) The soil groups: distribution, properties, classification, genesis and use. In: Fey M (ed) Soils of South Africa. Cambridge University Press, Singapore, pp 17–148

Foster IDL (2006) Lakes and reservoirs in the sediment delivery system: reconstructing sediment yields. In: Owens PN, Collins A (eds) Soil erosion and sediment redistribution in river catchments: measurement, modelling and management. CAB International, Wallingford, pp 128–142

Foster IDL, Lees JA, Owens PN, Walling DE (1998) Mineral magnetic characterization of sediment sources from an analysis of lake and floodplain sediments in the catchments of the Old Mill reservoir and Slapton Ley, South Devon, UK. Earth Surf Process Landforms 23: 685–703

Foster IDL, Boardman J, Keay-Bright J, Meadows M (2005) Land degradation and sediment dynamics in the South African Karoo. In: Horowitz JA, Walling DE (eds) Sediment budgets 2, IAHS Publ 292, IAHS, Wallingford, pp. 207–213.

Foster IDL, Boardman J, Keay-Bright J (2007) Sediment tracing and environmental history for two small catchments, Karoo Uplands, South Africa. Geomorphol 90:126–143

Foster IDL, Oldfield F, Flower RJ, Keatings K (2008) Mineral magnetic signatures in a long core from Lake Qarun, Middle Egypt. J Paleolimnol 40:835–849

Foster IDL, Collins AL, Naden PS, Sear DA, Jones JI, Zhang Y (2011) The potential for paleolimnology to determine historic sediment delivery to rivers. J Paleolimnol 45:287–306

Hancock G, Pietsch T (2008) Tracing and dating techniques employed at CSIRO land and water. CSIRO Science Report 64/08, CSIRO, Canberra

Lees JA (1994) Modelling the magnetic properties of natural and environmental materials. Unpublished PhD thesis, Coventry University, UK

Lees JA (1997) Mineral magnetic properties of mixtures of environmental and synthetic materials: linear additivity and interaction effects. Geophys J Int 131:335–346

Maher BA (1986) Characterisation of soils by mineral magnetic measurements. Phys Earth Planet Intern 42:76–92

Manjoro M (2012) Soil erosion and sediment source dynamics of a catchment in the eastern Cape Province, South Africa: an approach using remote sensing and sediment source fingerprinting techniques. Unpublished PhD thesis, Nelson Mandela Metropolitan University, Port Elizabeth, South Africa

Mucina L, Hoare DB, Lotter MC, Du Preez PJ, Rutherford MC, Scott-Shaw CR, Bredenkamp GJ, Powrie LW, Scott L, Camp GT, Cilliers SS, Bezuidenhout H, Mostert TH, Siebert SJ, Winter PJD, Burrows JE, Dobson L, Ward RA, Stalmans M, Oliver EGH, Siebert F, Schmidt E, Kobisi K, Kose L (2006) Grassland biome. In: Mucina L, Rutherford MC (eds) The vegetation of South Africa, Lesotho and Swaziland. South African National Biodiversity Institute, Pretoria, pp 349–431

Mzobe P (2014) Sediment linkages in a small catchment in the Mount Fletcher southern Drakensberg region, Eastern Cape, South Africa. Unpublished MSc thesis, Rhodes University, South Africa

Nel W (2008) Observations on daily rainfall events in the KwaZulu-Natal Drakensberg. Water SA 34:271–274

Nel W, Reynhardt D, Sumner P (2010) Effect of altitude on erosive characteristics of concurrent rainfall events in the northern KwaZulu-Natal Drakensberg. Water SA 36:509–512

Oldfield F (1999) The rock magnetic identification of magnetic mineral and magnetic grain size assemblages. In: Walden J, Oldfield F, Smith J (eds) Environmental magnetism: a practical guide. Quaternary Research Association, London, pp 98–112

Parsons AJ, Foster IDL (2011) What can we learn about soil erosion from the use of ^{137}Cs? Earth-Sci Rev 108:101–113

Partridge TC, Dollar E, Moolman J, Dollar L (2010) The geomorphic provinces of South Africa, Lesotho and Swaziland: a physiographic subdivision for earth and environmental scientists. T Roy Soc S Afr 65:1–47

Rowntree K, Foster I (2012) A reconstruction of historical changes in sediment sources, sediment transfer and sediment yield in a small, semi-arid Karoo catchment, semi-arid South Africa. Z Geomorphol 56:87–100

Rowntree KM, Mzobe P, van der Waal B (2012) Sediment source tracing in the Thina catchment, Eastern Cape, South Africa. In: Collins AL, Golosov V, Horowitz AJ, Lu, X, Stone M, Walling D, Zhang X (eds) Erosion and sediment yields in the changing environment, IAHS Publ 356, IAHS, Wallingford, pp. 404–411

Saint-Laurent D, Lavoie L, Drouin A, St-Laurent J, Ghaleb B (2010) Floodplain sedimentation rates, soil properties and recent flood history in southern Québec. Global Planet Change 70:76–91

Saxena DP, Joos P, Grieken RV, Subramanian V (2002) Sedimentation rate of the floodplain sediments of the Yamuna river basin (tributary of the river Ganges, India) by using ^{210}Pb and ^{137}Cs techniques. J Radioanal Nucl Ch 251:399–408

Smith HG, Blake WH (2014) Sediment fingerprinting in agricultural catchments: a critical re-examination of source discrimination and data corrections. Geomorphol 204:177–191

van der Waal B (2014) Sediment connectivity in the upper Thina catchment, Eastern Cape, South Africa. Unpublished PhD thesis, Rhodes University, South Africa

Walden J (1999) Remanence measurements. In: Walden J, Oldfield F, Smith J (eds) Environmental magnetism: a practical guide. Quaternary Research Association, London, pp 63–88

Wallbrink PJ, Murray AS, Olley JM, Olive LJ (1998) Determining sources and transit times of suspended sediment in the Murrumbidgee River, New South Wales, Australia, using fallout ^{137}Cs and ^{210}Pb. Water Resour Res 34:879–887

Walling DE (1999) Linking land use, erosion and sediment yields in river basins. In: Garnier J, Mouchel J-M (eds) Man and river systems. Springer, Dordrecht, pp 223–240

Walling DE (2004) Using environmental radionuclides to trace sediment mobilization and delivery in river basins as an aid to catchment management. Proceedings of the Ninth International Symposium on River Sedimentation October 18–21, Yichang, China, pp 121–135

Walling DE (2005) Tracing suspended sediment sources in catchments and river systems. Sci Total Environ 344:159–184

Walling DE (2013) The evolution of sediment source fingerprinting investigations in fluvial systems. J Soils Sediments 13:1658–1675

Walling D, Woodward J (1995) Tracing sources of suspended sediment in river basins: a case study of the River Culm, Devon, UK. Mar Freshwater Res 46:327–336

Walling DE, Peart MR, Oldfield F, Thompson R (1979) Suspended sediment sources identified by magnetic measurements. Nature 281: 110–113

Yu L, Oldfield F (1989) A multivariate mixing model for identifying sediment source from magnetic measurements. Quaternary Res 32: 168–181